GRAPHICAL MODELS AND IMAGE PROCESSING
Vol. 60, No. 1, January, pp. 57–76, 1998
ARTICLE NO. IP970455

Maximum Segmented Image Information Thresholding

C. K. Leung[1]

Department of Electronic Engineering, The Hong Kong Polytechnic University, Hung Hom, Kowloon, Hong Kong

and

F. K. Lam[2]

Department of Electrical and Electronic Engineering, The University of Hong Kong, Pokfulam Road, Hong Kong

Received October 2, 1995; revised September 25, 1997; accepted October 6, 1997

Utilizing information theory and considering image segmentation from a communication perspective, the image segmentation process is interpreted as a data processing step that operates on a gray-scale image and produces a segmented image. It is shown that the segmented image contains a certain amount of information about the scene, which is defined as *segmented image information* (SII). It is proposed that the SII should be maximized when an image is thresholded, and this is known as the *maximum segmented image information* (MSII) thresholding criterion. The MSII thresholding criterion possesses better properties as compared with the *minimum error* (MINE) and the *uniform error* (UNFE) thresholding criteria. Based on the MSII thresholding criterion, an MSII thresholding algorithm is proposed for the thresholding of real images. The MSII thresholding algorithm is evaluated against several well-known thresholding algorithms. The good thresholding results of both synthetic and real images confirm the capabilities of the proposed MSII thresholding algorithm. © 1998 Academic Press

1. INTRODUCTION

An image is a representation of a scene that consists of a set of spatially ordered picture elements (pixels). By observing the image, an observer will derive information about the scene. In view of this information transfer process, it will be useful to liken an image processing system to a communication system in which information is communicated from a source to a sink over a medium [1], as shown in Fig. 1 (the meanings of the terms H(X), GII, and SII will be discussed fully in the next section). The source of information is a scene. The medium is the collection of the image-capturing system, the gray-scale image, and the image-processing system. The sink is an observer that makes use of the output from the medium, which is the processed image. The sink could be another image-processing system, an image-understanding system, or even a human being. The information to be communicated to the observer is closely related to the observer's mission. For instance, if the observer is to decide on the presence or absence of a certain object at the scene, the information to be transferred should be about whether the pixels belong to that object or not. In this case, a segmented image will be generated from the gray-scale image and presented to the observer.

Image segmentation is an important step toward higher level image-processing stages such as feature extraction, pattern recognition, and classification [2]. By virtue of its high speed of operation and simplicity in implementation, thresholding has been the most popular approach to image segmentation and has been reviewed extensively in the literature [3]. In recent years, a number of thresholding methods based on the information-theoretic concept of entropy have been proposed [4–15]. In what follows, we will categorize these entropic thresholding algorithms into two groups according to how the entropy concept is being utilized. To bring out their similarities and differences, algorithms belonging to the same group will be reviewed collectively.

Entropic thresholding algorithms in the first group consider the thresholded image as a collection of two or more objects each having a probability of occurrence. Since these probabilities pertain to objects generated after thresholding, they are known as the *a posteriori* probabilities. Based on these *a posteriori* probabilities some *a posteriori* entropy measures may be defined. Each algorithm in this group maximizes the *a posteriori* entropy in one form or another with different additional constraints. Pun [4] derives an upper bound of the *a posteriori* entropy from knowledge of the histogram and maximizes this upper bound. Wong *et al.* [5] maximize simultaneously the *a posteriori* entropy, the uniformity, and the shape measures of the image. In this way, structural information of the image has been incorporated into thresholding. Pal and Pal [6] utilize spatial information of the

[1] To whom correspondence should be addressed. E-mail: enchikin@polyu.edu.hk.

[2] E-mail: fklam@hkueee.hku.hk.

1077-3169/98 $25.00
Copyright © 1998 by Academic Press
All rights of reproduction in any form reserved.

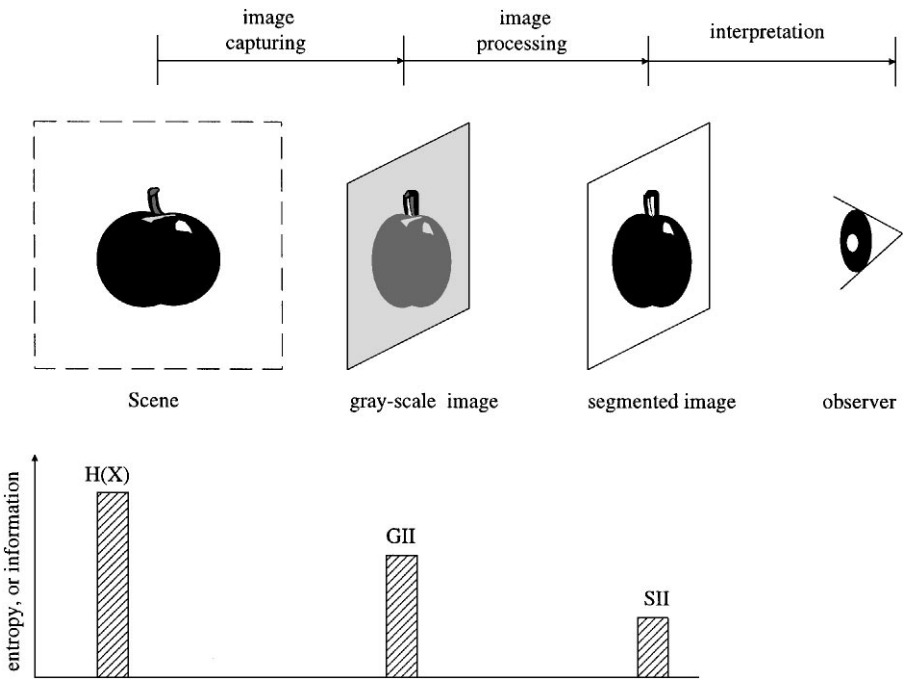

FIG. 1. Image-processing stages and information.

image by considering the probability density function (pdf) of the joint gray-level distribution of two neighboring pixels taken at a time and maximize the *a posteriori* entropy of the thresholded pdf. This method is further developed by Pal and Pal [7] with a new definition of entropy in an exponential form for calculating the *a posteriori* entropy. A recent method by Beghdadi *et al.* [8] incorporates spatial information to a greater extent by considering the pdf of pixel blocks in $m \times n$ size.

Entropic thresholding algorithms in the second group consider the thresholded image as two classes of events with each class being characterized by a pdf. Usually each event represents a pixel assuming a certain gray-level value or two neighboring pixels assuming a joint gray-level values pair. The method by Johannsen and Bille [9] minimizes the interdependence between the two classes. The method by Kapur *et al.* [10] maximizes the sum of the entropy of the two pdfs that results from thresholding. Kapur's method is adapted by Abutaleb [11] to maximize the 2D entropy. In this case, the pdf of the joint occurrence of the gray-level value of a pixel and the average of the gray-level values of its neighborhood pixels is thresholded and the sum of their entropies is maximized. In a method by Brink [12], Kapur's sum-of-entropy maximization strategy is employed where the two normalized autocorrelation functions of the thresholded histogram are taken to be the two pdfs for entropy calculation. Li and Lee [13] minimize the Kullback–Leibler distance between the pdf of the original image and the pdf of the thresholded image. Chang *et al.* [14] minimize the Kullback–Leiber distance between the pdf of the original image and the thresholded pdf of neighboring pixels taken two at a time. This method effectively takes into account some structural information of the image. Lam and Leung [15] maximize the entropy of the image pdf and come up with a quasi-Gaussian image model for the implementation of an iterative maximum likelihood segmentation algorithm.

Most of these information-theoretic thresholding methods have been proposed on an *ad hoc* basis with many details left unexplained, as has been commented by some authors [9]. In this paper, we shall place the information-theoretic thresholding theory on a more logical foundation by viewing the thresholding process in a communication perspective. Thresholding is interpreted as a data-processing step that outputs a thresholded image which contains a certain amount of information about the scene. We propose to use a thresholding criterion that maximizes the amount of information contained in a thresholded image so that its observer is given the maximum amount of information about the scene. It will be shown that both the *a posteriori* entropy and the *a priori* information about the image will be used to generate such a thresholded image, thus a better thresholding result will be achieved. This method is referred to as *maximum segmented image information* (MSII) thresholding. The rest of this paper is organized as follows. In Section 2, the theory of MSII thresholding is developed. In Section 3, the properties of the MSII thresholding criterion are analyzed and compared to two error-based thresholding criteria, namely the *minimum error* (MINE) and the *uniform error* (UNFE) criteria. In Section 4, an MSII thresholding algorithm for thresholding real images is proposed. The thresholding results of a large number of synthetic and real images are discussed. In Section 5, the extension of the MSII

criterion to multiclass segmentation is discussed. In Section 6, a conclusion is given.

2. THEORY

2.1. Notations

Without loss of generality, we shall consider a scene that consists of an object in a background whereas the general case of multiple objects in a background will be discussed in Section 5. Assume that an imaging system captures a gray-scale image with N pixels about the scene. We also assume that the number of pixels from the object part is αN and that from the background part is $(1-\alpha)N$, with $0<\alpha<1$. Denote a pixel as X and its gray-level value as g, where $g \in \{0, 1, \ldots, L-1\}$; i.e., the gray-level values of the gray-scale image are discretized into L levels ranging from 0 to $L-1$ in unit step.

The probability density function (pdf) of the gray-level values of the object pixels is denoted as $P(\text{gray level} = g | X \in F_0) = f_0(g)$. Similarly, the pdf of the gray-level values of the background pixels is denoted as $P(\text{gray level} = g | X \in F_1) = f_1(g)$. The pdf of the composite image is denoted as $P(\text{gray level} = g | X \in F) = f(g)$. It is easily shown that $f(g)$ is related to $f_0(g)$ and $f_1(g)$ by

$$f(g) = \alpha f_0(g) + (1-\alpha) f_1(g). \tag{1}$$

F_0, F_1, and F are the sets of object pixels, background pixels, and composite image pixels, respectively.

2.2. Scene Entropy

Consider that a scene is represented by an image of N pixels. If pixel X is selected from the image at random, the probability that X belongs to the object part is α, and the probability that it belongs to the background part is $(1-\alpha)$, i.e.,

$$P(X \in F_0) = \alpha, \quad P(X \in F_1) = 1-\alpha. \tag{2}$$

According to Shannon [1], the uncertainty about which part (i.e., object or background) X belongs to is measured by the entropy expression

$$H(X) = -\alpha \log(\alpha) - (1-\alpha)\log(1-\alpha) = H_2[\alpha, 1-\alpha]. \tag{3}$$

We employ the notation $H_n[p_1, p_2, \ldots, p_n] = -\sum_{i=1}^{n} p_i \log(p_i)$ to represent the entropy of a probability distribution $\{p_1, p_2, \ldots, p_n\}$. Unless specified otherwise, the $\log(\cdot)$ notation denotes logarithm to base 2. The unit of the uncertainty measure in Eq. (3) is bits/pixel, which has been omitted for brevity. Equation (3) denotes the average uncertainty about the classification status of an image pixel of a scene without regard to any other information. We define the expression $H(X)$ as *scene entropy*. It is anticipated that if other information about the scene is available, this uncertainty will drop to a lower value.

2.3. Gray-Scale Image Information (GII)

Consider that a gray-scale image consisting of N pixels has been captured to represent the scene. Suppose that an observer of this gray-scale image has observed a gray-level value of g for pixel X. The *a posteriori* probability that pixel X belongs to the object part is

$$P(X \in F_0 \mid g) = \frac{\alpha f_0(g)}{f(g)}. \tag{4}$$

Similarly, the *a posteriori* probability that pixel X belongs to the background part is

$$P(X \in F_1 \mid g) = \frac{(1-\alpha) f_1(g)}{f(g)}. \tag{5}$$

Conditioned on the observed gray-level value g, the uncertainty about which part pixel X belongs to is

$$H(X \mid g) = H_2\left[\frac{\alpha f_0(g)}{f(g)}, \frac{(1-\alpha) f_1(g)}{f(g)}\right]. \tag{6}$$

The average uncertainty for the entire image is given by the weighted sum of $H(X \mid g)$

$$H(X \mid G) = \sum_{g=0}^{L-1} f(g) H_2\left[\frac{\alpha f_0(g)}{f(g)}, \frac{(1-\alpha) f_1(g)}{f(g)}\right]. \tag{7}$$

With some mathematical manipulation, $H(X \mid G)$ in Eq. (7) may be written as

$$H(X \mid G) = H(X) + \alpha H(F_0) + (1-\alpha) H(F_1) - H(F), \tag{8}$$

where the notations $H(F_0)$, $H(F_1)$, and $H(F)$ represent the entropy of the probability distribution $f_0(g)$, $f_1(g)$, and $f(g)$ for $g \in \{0, 1, \ldots, L-1\}$, respectively. For instance, $H(F_0)$ is computed as $-\sum_{g=0}^{L-1} f_0(g) \log f_0(g)$. $H(X \mid G)$ represents the *residual uncertainty* about the pixel classification after the gray-scale image has been observed. Similar to the way in which mutual information is defined in information theory [16], we define the *gray-scale image information* (GII) as the reduction in uncertainty about the pixels' classification after the gray-scale image has been observed, as in

$$\begin{aligned} \text{GII} &\equiv \text{initial uncertainty} - \text{residual uncertainty} \\ &= H(X) - H(X \mid G) \\ &= H(F) - \alpha H(F_0) - (1-\alpha) H(F_1). \end{aligned} \tag{9}$$

The unit of GII is bits/pixel, which has been omitted from Eq. (9) for brevity.

2.4. Segmented Image Information (SII)

Utilizing information theory [17], binary image segmentation may be viewed as a data-processing step that classifies (or segments) the image pixels into either class C_0 (i.e., $X \to C_0$), or class C_1 (i.e., $X \to C_1$). For the moment, we assign no semantic meaning to class C_0 or C_1.

Suppose that the segmented image is presented to an observer. If a particular pixel has been segmented into class C_0, the *a posteriori* probability that it actually belongs to the object part is the conditional probability $P(X \in F_0 \mid X \to C_0)$. By *Bayes'* theorem, this can be written as

$$P(X \in F_0 \mid X \to C_0) = \frac{P(X \in F_0)\, P(X \to C_0 \mid X \in F_0)}{P(X \to C_0)} = \frac{\alpha P_{00}}{P_0}. \tag{10}$$

Here we have employed the notation P_{ij} to denote $P(X \to C_i \mid X \in F_j)$, and the notation P_i to denote $P(X \to C_i)$ for $i,\ j = 0, 1$. Similarly, the *a posteriori* probability that the pixel actually belongs to the background part under the same condition is given by

$$P(X \in F_1 \mid X \to C_0) = \frac{(1-\alpha)P_{01}}{P_0}. \tag{11}$$

Since $\alpha P_{00} + (1-\alpha)P_{01} = P_0$, it may be verified that the sum of these two *a posteriori* probabilities is 1.

For all those pixels that have been segmented into class C_0, the average uncertainty about their actual classification is

$$H(X \mid X \to C_0) = H_2\left[\frac{\alpha P_{00}}{P_0}, \frac{(1-\alpha)P_{01}}{P_0}\right]. \tag{12}$$

Similarly, for all those pixels that have been segmented into class C_1, the average uncertainty about their actual classification is

$$H(X \mid X \to C_1) = H_2\left[\frac{\alpha P_{10}}{P_1}, \frac{(1-\alpha)P_{11}}{P_1}\right] \tag{13}$$

We denote the average uncertainty about a pixel's classification as $H(X \mid C)$, which is given by the weighted sum of $H(X \mid X \to C_0)$ and $H(X \mid X \to C_1)$, as

$$H(X \mid C) = P_0 H(X \mid X \to C_0) + P_1 H(X \mid X \to C_1). \tag{14}$$

The value of $H(X \mid C)$ in Eq. (14) represents the average *residual uncertainty* about which class a pixel belongs to after the segmented image has been observed. In a way similar to defining the gray-scale image information, we define the *segmented image information* (SII) as the reduction in uncertainty, as in

$$\begin{aligned}\text{SII} &\equiv H(X) - H(X \mid C) \\ &= H(X) - P_0 H(X \mid X \to C_0) - P_1 H(X \mid X \to C_1).\end{aligned} \tag{15}$$

With some mathematical manipulation, SII in Eq. (15) may be written as

$$\text{SII} = H_2[P_0, 1-P_0] - \alpha H_2[P_{00}, P_{10}] - (1-\alpha)H_2[P_{01}, P_{11}]. \tag{16}$$

The unit of SII is bits/pixel, which has been omitted from Eqs. (15) and (16) for brevity.

From standard results of information theory, which deal with the change of information by data processing [17], it may be shown that the following inequality about scene entropy, GII, and SII is valid:

$$H(X) \geq \text{GII} \geq \text{SII}. \tag{17}$$

It is to be noted that inequality (17) can be proved by using Eqs. (3), (9), and (16). The general relationship between these three terms is illustrated in Fig. 1. SII is bounded by GII, as well as by $H(X)$. If GII is small, SII will also be small no matter what segmentation algorithm is employed so long as only the gray-level values of the gray-scale image pixels are inspected in isolation. Hence for good segmentation results to be possible, GII should be large and as close to $H(X)$ as is practically allowed. In practice, a large value of GII may be ensured during the image acquisition stage, for instance, by maintaining good contrast between the object and the background with good lighting conditions. But after the gray-scale image has been formed, it is not possible to increase the GII, and hence the upper bound of the SII will remain fixed. This implies the best possible performance of image segmentation, in an information-theoretic sense, is fixed once the gray-scale image has been acquired. The GII of a gray-scale image is a useful index to quantify its suitability for segmentation. The SII of a segmented image is a useful index to quantify its goodness as a representation of the original scene.

2.5. SII of Some Special Segmented Images

With the segmented image information defined above, a segmented image can be assessed in terms of the SII—the greater the SII, the better is the segmented image in an information-theoretic sense. To illustrate the properties of the SII and its suitability for segmented image assessment, the SII of several special segmented images are considered. The SII is compared to the segmentation error rate E, which is the ratio of the number of wrongly segmented pixels to the total number of image pixels N. Note that if the scene entropy is $H(X)$, the SII will lie within a range of $[0,\ H(X)]$, while the segmentation error rate E will lie within a range of [0, 1]. With these two performance indices, a large SII or a small segmentation error rate indicates a good segmented image, while a small SII or a large segmentation error rate indicates a bad segmented image. In calculating the SII values for the following special cases, we shall assume that object pixels and black color are denoted as "0," and that background pixels and white color are denoted as "1." The relative size of

the object pixels is α of the entire image. The normally correct segmentation rule is such that object pixels are segmented into black and background pixels are segmented into white.

The first case to be considered is a perfectly segmented image, where all image pixels are segmented correctly. In this case, $P_0 = \alpha$, $P_1 = 1-\alpha$, $P_{00} = 1$, $P_{10} = 0$, $P_{01} = 0$, and $P_{11} = 1$. According to Eqs. (16) and (3), SII $= H_2[P_0, 1-P_0] - \alpha H_2[1, 0] - (1-\alpha)H_2[0, 1] = H_2[\alpha, 1-\alpha] = H(X)$. Hence the SII is equal to the scene entropy $H(X)$. This value is the maximum within the range $[0, H(X)]$. The segmentation error rate E is 0, which is the smallest value within the range [0, 1]. Hence a perfectly segmented image will be rated the *best* by both the SII and the segmentation error rate *E*. Both results are reasonable.

The second case to be considered is a randomly segmented image, which is produced by segmenting each image pixel randomly without regard to any observation information. To calculate the SII, we assume that the probability of segmenting any image pixel into black color is β, where $0 \le \beta \le 1$, and that the probability of segmenting into white color is $1-\beta$. In this case, $P_0 = \beta$, $P_1 = 1-\beta$, $P_{00} = \beta$, $P_{10} = 1-\beta$, $P_{01} = \beta$, and $P_{11} = 1-\beta$. According to Eq. (16), SII $= H_2[\beta, 1-\beta] - \alpha H_2[\beta, 1-\beta] - (1-\alpha)H_2[\beta, 1-\beta] = H_2[\beta, 1-\beta](1-\alpha-(1-\alpha)) = 0$. Hence the SII for this case is 0, which is the minimum in the range $[0, H(X)]$ and will rate a randomly segmented image the *worst*. If the image is to be segmented into an object and a background randomly, the segmentation error rate E will be $\alpha(1-\beta)+(1-\alpha)\beta$. This value may be small or large depending on the actual values of α and β. In particular, if $\beta = 1/2$, the segmentation error rate will be 0.5. Then the segmentation error rate E will rate a randomly segmented image *quite poor*, or *quite good*, but not the *worst*. In this case, the segmentation error rate E is not as effective as the SII to indicate that a randomly segmented image is the *worst* segmented image.

The third case to be considered is a purely black (or purely white) segmented image. Consider a purely black segmented image, $P_0 = 1$, $P_1 = 0$, $P_{00} = 1$, $P_{10} = 0$, $P_{01} = 1$, and $P_{11} = 0$. According to Eq. (16), SII $= H_2[1, 0] - \alpha H_2[1, 0] - (1-\alpha)H_2[1, 0] = 0 - 0 - 0 = 0$. The case of the purely white segmented image is similar. Hence the SII is 0, which is the minimum in the range $[0, H(X)]$ and will rate a purely black (or purely white) segmented image the *worst*. If the segmentation process is designed such that an object pixel is to be segmented into black color and a background pixel into white color, then a purely white segmented image has a segmentation error rate equal to α, where α is the size of the object relative to the entire image. The error rate may be small or large depending on the actual value of α. If α is small, a small segmentation error rate will be obtained and the purely white segmented image will be rated *good*. This is a misleading indication, since a purely white image would be of no value for any subsequent image processing step as far as the scene content is concerned. In this case, the segmentation error rate is not as effective as the SII to rate a purely white (or purely black) segmented image the *worst*.

The fourth case to be considered is a segmented image which has been produced in the "reverse color;" i.e., all object pixels are segmented into white color and all background pixels are segmented into black color. In this case, all pixels have been segmented wrongly and the segmentation error rate is 1. Hence the segmentation error rate will rate such a "reverse color" segmented image the *worst*. To calculate the SII, we note that $P_0 = 1-\alpha$, $P_1 = \alpha$, $P_{00} = 0$, $P_{10} = 1$, $P_{01} = 1$, and $P_{11} = 0$. According to Eq. (16), SII $= H_2[1-\alpha, \alpha] - \alpha H_2[0, 1] - (1-\alpha) H_2[1, 0] = H(X) - 0 - 0 = H(X)$. Hence the SII of this segmented image is equal to the scene entropy $H(X)$, which is the maximum value in the range $[0, H(X)]$. This result indicates that such a segmented image is rated the *best* by SII. This is a more reasonable result since a "reverse color" segmented image possesses all the details (such as object shape, object location, object size) about the scene and hence will be equivalent to the original scene.

Considering these special segmented images, it is found that SII is a better index to assess a segmented image than the segmentation error rate. Subsequently, a thresholding criterion which maximizes the SII (to be discussed in the following) is expected to perform better than a criterion which minimizes the segmentation error rate.

2.6. MSII Thresholding Criterion

Given a threshold value $k \in \{-1, 0, 1, \ldots, L-1\}$, a pixel that has a gray-level value smaller than or equal to k will be thresholded into class C_0, otherwise the pixel is thresholded into class C_1. When $k = -1$, all pixels of the image will be thresholded into class C_1. When $k = L-1$, all pixels will be thresholded into class C_0. In general an image can be thresholded in a total of $L+1$ different ways with $L+1$ different threshold values. Without loss of generality, we will assume that by thresholding a pixel to class C_0 (or C_1), it is purported that this pixel is an object (or a background) pixel. Hence P_{10} is the error probability of thresholding an object pixel. In the context of object detection, this is a kind of misdetection, which may be called a miss, or type I error [18]. We shall denote this error as $E1$; i.e.,

$$E1 = P_{10}. \tag{18}$$

Similarly, P_{01} is the error probability of thresholding a background pixel. Also, in the context of object detection, this is a kind of misdetection, which may be called a false alarm or a type II error [18]. We shall denote this error as $E2$; i.e.,

$$E2 = P_{01}. \tag{19}$$

The total error probability E of thresholding the image is given by

$$E = \alpha E1 + (1-\alpha)E2. \tag{20}$$

In terms of these error probabilities, SII in Eq. (16) may be

written as

$$\mathrm{SII} = H_2[P_0, 1-P_0] - \alpha H_2[1-E1, E1] - (1-\alpha)H_2[E2, 1-E2]. \tag{21}$$

It is interesting to note that the terms P_{01} and P_{10} are in meaning similar to the confusion matrix elements that have been utilized in formulating a criterion for thresholding an image for the sake of edge detection [19].

In the information-theoretic sense, the larger the SII, the better will be the segmented image, since it contains more information about the original scence. Hence a possible criterion in choosing the best threshold value is to maximize the SII. This thresholding criterion is called the *maximum segmented image information* (MSII) thresholding criterion. The optimum threshold value so chosen is denoted as k_{MSII}, which may be determined as

$$k_{\mathrm{MSII}} = \arg \max_{k\in\{-1,0,1,\ldots,L-1\}} \mathrm{SII}_k, \tag{22}$$

where SII_k has been used in place of SII to highlight its k-dependent feature.

Since all three terms in the right-hand side of Eq. (21) are positive, the MSII thresholding criterion may be interpreted as one of striking a compromise between maximizing $H_2[P_0, 1-P_0]$ and minimizing $\alpha H_2[1-E1, E1]$ and $(1-\alpha)H_2[E2, 1-E2]$. Maximizing the term $H_2[P_0, 1-P_0]$ thresholds the image into two classes of pixels as similar in size as possible. In general, minimizing the term $\alpha H_2[1-E1, E1]$ may be accomplished in two different ways. The first is to minimize the error probability $E1$. The second is to make $E1$ as near to 1 as possible. The first approach will result in a small segmentation error rate and hence is adopted in many thresholding algorithm designs. The second approach will result in a large segmentation error rate. Since this is equivalent to the case of "reverse color" segmentation as discussed in the previous section, the thresholding result is also good in an information-theoretic sense. As for minimizing the term $(1-\alpha)H_2[E2, 1-E2]$, similar discussions apply with $E1$ replaced by $E2$. In practical thresholding, it will not be possible to minimize $E1$ and $E2$ simultaneously or make them near to 1 simultaneously. Hence the SII is to be minimized by making a compromise.

To relate the proposed MSII thresholding criterion to some previous works in thresholding, it would be interesting to note that many thresholding algorithms aim at maximizing $H_2[P_0, 1-P_0]$ or minimizing the segmentation error rate in isolation, but not jointly as proposed here in the MSII thresholding criterion. Kittler–Illingworth's method aims at minimizing the segmentation error rate [21]. Maximizing $H_2[P_0, 1-P_0]$ in isolation will give the trivial solution of thresholding the image into two classes in equal size. Many thresholding algorithms try to avoid such a trivial solution by incorporating extra rules. Pun's method maximizes the upper bound of $H_2[P_0, 1-P_0]$ instead of $H_2[P_0, 1-P_0]$ itself [4]. Wong *et al.* maximize $H_2[P_0, 1-P_0]$ together with the uniformity and shape measure of the segmented image [5]. Pal and Pal maximize a two-dimensional version of $H_2[P_0, 1-P_0]$ [7]. Beghdadi *et al.* adopt a similar approach but consider thresholded pixels in an $m \times n$ neighborhood block [8].

3. PROPERTIES OF THE MSII THRESHOLDING CRITERION

3.1. MSII Thresholding Criteria Comparison

To investigate the properties of the MSII thresholding criterion, it will be useful to compare it with other thresholding criteria. We adopt two thresholding criteria, namely the *minimum error* (MINE) and the *uniform error* (UNFE) criterion. MINE minimizes the total error E as specified in Eq. (20) and has been employed by Kittler and Illingworth in designing a practical thresholding algorithm [21]. UNFE equalizes the two error probabilities $E1$ and $E2$ and has been employed by Dunn *et al.* [20]. If the original scene is known, the threshold values satisfying the MINE and UNFE criteria can be computed and are denoted as k_{MINE} and k_{UNFE}, respectively. We will refer to threshold values obtained in this way as *ideal* threshold values, where they can be computed as

$$k_{\mathrm{MINE}} = \arg \min_{k\in\{-1,0,1,\ldots,L-1\}} E_k \tag{23}$$

$$k_{\mathrm{UNFE}} = \arg \min_{k\in\{-1,0,1,\ldots,L-1\}} |E1_k - E2_k|. \tag{24}$$

E_k, $E1_k$, and $E2_k$ have been written in place of E, $E1$, and $E2$, respectively, to highlight their k-dependent feature.

3.2. Thresholding Properties Evaluation

For the purpose of formulating thresholding algorithms and evaluating their performance, it is common to assume a Gaussian form for the two subimage pdfs $f_0(g)$ and $f_1(g)$ [21–24]. We will follow the same approach by assuming

$$f_0(g) = N(\mu_0, \sigma_0; g) = \frac{1}{\sigma_0\sqrt{2\pi}} \exp\left[\frac{-(g-\mu_0)^2}{2\sigma_0^2}\right] \tag{25}$$

$$f_1(g) = N(\mu_1, \sigma_1; g) = \frac{1}{\sigma_1\sqrt{2\pi}} \exp\left[\frac{-(g-\mu_1)^2}{2\sigma_1^2}\right]. \tag{26}$$

The image pdf $f(g)$ is related to $f_0(g)$ and $f_1(g)$ according to Eq. (1). Based on this image model, the three ideal threshold values k_{MSII}, k_{MINE}, and k_{UNFE} can be obtained according to Eqs. (22), (23), and (24), respectively, once the 5-tuple parameters $(\alpha, \mu_0, \sigma_0, \mu_1, \sigma_1)$ are specified.

To compare the MSII thresholding criteria with the MINE and UNFE criteria, we determine the three ideal threshold values for each image from a set of synthetic images modeled above. Since all the three thresholding criterion under comparison only require the knowledge of α, $f_0(g)$, and $f_1(g)$ to determine the corresponding ideal threshold values, there is no need to synthesize the actual image. Instead, only the 5-tuple parameters

$(\alpha, \mu_0, \sigma_0, \mu_1, \sigma_1)$ are specified, and then the subimage pdfs $f_0(g)$ and $f_1(g)$ are synthesized according to Eqs. (25) and (26), respectively. With α, $f_0(g)$, and $f_1(g)$ known exactly, the three ideal threshold values can be determined. Since no actual image has been synthesized, each case of synthetic image will be referred to as an *ideal pdf*.

To cater for a wide range of image characteristics, various combinations in the 5-tuple parameters have been employed to generate the ideal pdfs. The value of α ranges from 0.1 up to 0.5 in steps of 0.05. Both σ_0 and σ_1 range, independently, from 10 to 50 in steps of 5. Without loss of generality, μ_1 is designed to be greater than μ_0. The separation of μ_0 and μ_1 ranges from 51 to 105 in steps of 6, with the value of $1/2(\mu_0 + \mu_1)$ fixed at 128.5. The gray-level value g ranges from 0 to 255, which is equivalent to an-8-bit resolution for a monochrome image. A total of 7290 ideal pdfs have been synthesized. For these 7290 ideal pdfs, the ideal threshold values k_{MINE}, k_{MSII}, and k_{UNFE} are obtained according to Eqs. (22), (23), and (24). Those ideal pdfs leading to an ideal MINE thresholding error E less than 0.01% are precluded from further investigation since the two pdfs, $f_0(g)$ and $f_1(g)$, are almost nonoverlapping that it would be trivial to threshold images with such pdfs. Finally, a total of 7181 ideal pdfs remain. Out of these 7181 ideal pdfs, 2904 of them are unimodal and 4277 of them are bimodal. It is to be noted that ideal pdfs with $\alpha > 0.5$ have not been synthesized. It is because the threshold value k, where k is one of k_{MINE}, k_{MSII}, and k_{UNFE}, of an ideal pdf with parameters $(\alpha, \mu_0, \sigma_0, \mu_1, \sigma_1)$ is related to the threshold value k' of the ideal pdf with parameters $(1 - \alpha, \mu_0, \sigma_1, \mu_1, \sigma_0)$ by $k = 255 - k'$. As a result, threshold values of ideal pdfs with $\alpha > 0.5$ may be derived from threshold values of ideal pdfs with $\alpha < 0.5$.

When the ideal threshold values k_{MINE}, k_{MSII}, and k_{UNFE} of the 7181 ideal pdfs are examined, the following observation can be made:

(i) All of the ideal MSII and UNFE threshold values lie within the [0, 255] dynamic range. However, 103 of the ideal MINE threshold values are equal to -1, which means that the MINE criterion thresholds all the pixels into one class only. Obviously, these results are not compatible with the *a priori* assumption that the image is made up of two subimages. To visualize the thresholding results in this situation, we actually synthesize a 512×512 image with parameters $(\alpha, \mu_0, \sigma_0, \mu_1, \sigma_1) = (0.2, 103, 20, 154, 45)$. The original scene is a circular object in a background. The object size is 0.2 of the total image size. The gray-level values of the object pixels and the background pixels are generated by a random number generation subroutine [25] which generates random integers that are normally distributed in the range 0 to 255. The mean gray-level value of the object pixels is 103, and the standard deviation is 20. The mean gray-level value of the background pixels is 154, and the standard deviation is 45. For this synthetic image, it is found that $k_{\text{MINE}} = -1$, $k_{\text{MSII}} = 135$, and $k_{\text{UNFE}} = 118$. The original scene, the synthetic gray-scale image, its histogram, and the MSII- and UNFE-thresholded images are shown in Figs. 2a–2e, respectively. The MINE-thresholded image is only a purely white image and hence is not shown. When the image is thresholded at the ideal MSII or UNFE threshold value, a circular object is still recognizable from the thresholded image. The pitfall of the MINE criterion compared with the MSII and UNFE criterion is illustrated by this example.

(ii) When $\sigma_0 = \sigma_1 = \sigma$ and $\alpha = 0.5$, it is observed that $k_{\text{MINE}} = k_{\text{MSII}} = k_{\text{UNFE}} = 1/2(\mu_0 + \mu_1)$ for all the images. Hence, it may be discovered that, within the present scope of investigation, MSII, MINE, and UNFE thresholding criteria are equivalent when the object and background have equal size and the standard deviation of the gray-level values of the object pixels and that of the background pixels are equal.

(iii) When $\sigma_0 = \sigma_1 = \sigma$ and $\alpha < 0.5$ it is observed that $k_{\text{MINE}} \leq k_{\text{MSII}} \leq k_{\text{UNFE}}$; i.e., the ideal MSII threshold values are found to lie between the MINE and UNFE threshold values. To visualize the thresholding results in this situation, we consider, as a special case, the thresholding of the ideal pdf defined by parameters $(\alpha, \mu_0, \sigma_0, \mu_1, \sigma_1) = (0.1, 88, 50, 169, 50)$. The three ideal threshold values are determined as $k_{\text{MINE}} = 118$, $k_{\text{MSII}} = 124$, $k_{\text{UNFE}} = 128$. Having obtained these threshold values, a 512×512 image that has a circular object against a background is synthesized by generating the pixel gray-level values according to a Gaussian distribution, as discussed above. The original scene, the synthesized gray-scale image, its histogram, and the three thresholded images are shown in Figs. 3a–3f, respectively.

(iv) For cases other than those discussed in Sections (i) to (iii) above, no definite relationship between the three threshold values can be observed. However, it is found that the root-mean-square difference between k_{MSII} and k_{MINE} is 12.93, that between k_{MSII} and k_{UNFE} is 11.34, and that between k_{MINE} and k_{UNFE} is 17.29. Hence on the average, the ideal MSII threshold values are found to lie close to the ideal MINE and UNFE threshold values.

4. MSII THRESHOLDING ALGORITHM AND RESULTS

In practical situations, only the image histogram $f(g)$ can be observed, neither the image model nor the associated parameters are known in advance. In order to determine the MSII threshold for an image, it is required that the individual pdfs of the subimages and the mixing ratio are known. For the purpose of thresholding a real image, the individual pdfs and the mixing ratio may be estimated and the segmented image information calculated. In this section, we propose a thresholding algorithm based on the MSII criterion, which is called *MSII thresholding algorithm*. This algorithm is similar to Kittler–Illingworth's algorithm [21] in that the image is assumed to be composed of subimages with Gaussian pdfs. The four parameters of the two Gaussian pdfs of the subimages μ_0, σ_0, μ_1, and σ_1, and the mixing ratio α, are estimated at some tentative threshold t. With these parameters estimated, the MSII threshold value can be determined. An

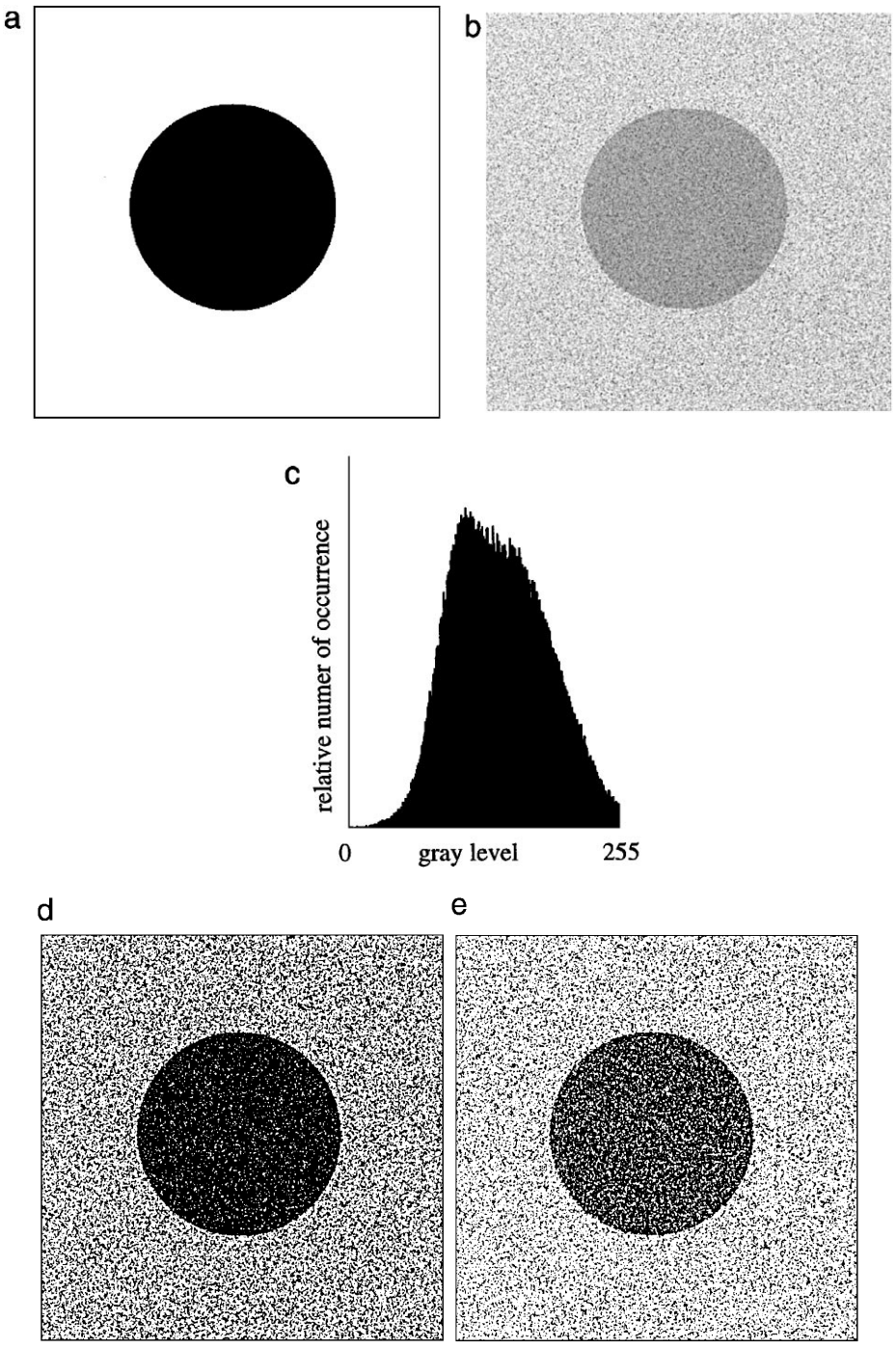

FIG. 2. Thresholding results for a synthetic image with parameters $\alpha = 0.2$, $\mu_0 = 103$, $\sigma_0 = 20$, $\mu_1 = 154$, $\sigma_1 = 45$: (a) original scene, (b) gray-scale image, (c) histogram, (d) thresholded by MSII criterion at 135, (e) thresholded by UNFE criterion at 118.

exhaustive search is performed on the entire gray-level value range to determine the optimum threshold value. In order not to have a zero value for the estimated parameters σ_0 or σ_1, the practical search range is from $t = 2$ up to $t = 253$ for a gray-level value range of 0 to 255. The MSII thresholding algorithm is formulated as follows:

Step 1 Initialize MaxSII $= -1$, $t = 2$, and $\hat{k}_{\text{MSII}} = 2$

Step 2 estimate the five parameters $(\hat{\alpha}, \hat{\mu}_0, \hat{\sigma}_0, \hat{\mu}_1, \hat{\sigma}_1)$ as follows:

$$\hat{\alpha} = \sum_{g=0}^{t} f(g),\ \hat{\mu}_0 = \frac{\sum_0^t g f(g)}{\hat{\alpha}},\ \hat{\sigma}_0^2 = \frac{\sum_0^t (g - \hat{\mu}_0)^2 f(g)}{\hat{\alpha}}$$

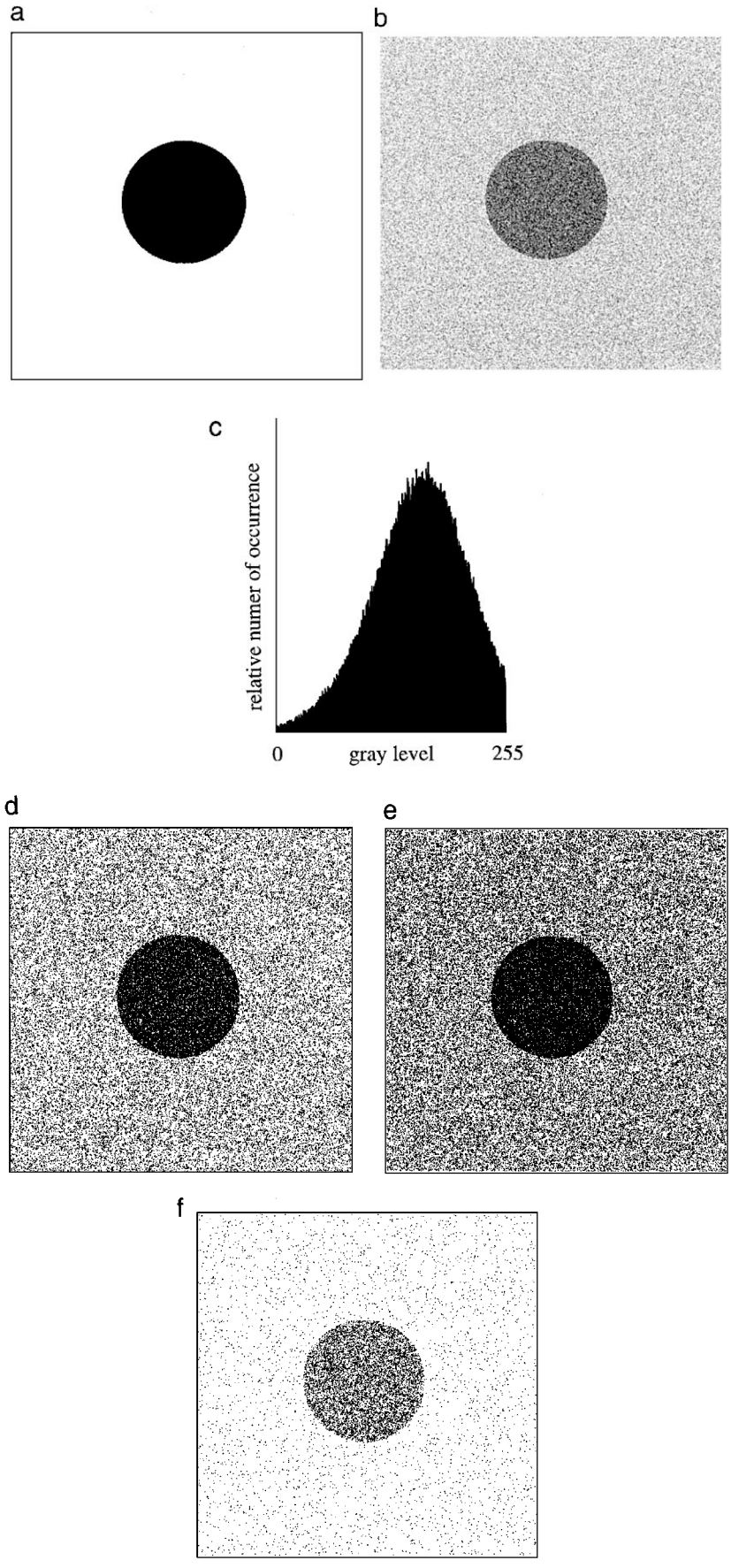

FIG. 3. Thresholding results for a synthetic image with parameters $\alpha = 0.1$, $\mu_0 = 88$, $\sigma_0 = 50$, $\mu_1 = 169$, $\sigma_1 = 50$: (a) original scene, (b) gray-scale image, (c) histogram, (d) thresholded by MSII criterion at 113, (e) thresholded by UNFE criterion at 128, (f) thresholded by MINE criterion at 60.

$$\hat{\mu}_1 = \frac{\sum_{t+1}^{L-1} g f(g)}{1-\hat{\alpha}}, \hat{\sigma}_1^2 = \frac{\sum_{t+1}^{L-1} (g-\hat{\mu}_1)^2 f(g)}{1-\hat{\alpha}}$$

Step 3 estimate $\hat{f}_0(g)$ as $N(\hat{\mu}_0, \hat{\sigma}_0; g)$

$$\text{estimate } \hat{f}_1(g) \text{ as } \frac{f(g)-\hat{\alpha}\hat{f}_0(g)}{1-\hat{\alpha}}, \text{ if } \hat{f}_1(g) < 0, \text{ set } \hat{f}_1(g) = 0$$

Step 4 assume that the true subimage pdfs are $\hat{f}_0(g)$ and $\hat{f}_1(g)$ and that they are mixed by the ratio $\hat{\alpha}$, i.e., the composite image pdf is given by $\hat{\alpha}\hat{f}_0(g) + (1-\hat{\alpha})\hat{f}_1(g)$, threshold this ideal pdf at t and estimate the segmented image information $\hat{\text{SII}}$ as:

$$\hat{\text{SII}} = H_2[P_0, 1-P_0] - \alpha H_2[1-E1, E1] - (1-\alpha)H_2[E2, 1-E2],$$

where P_0, α, $E1$, and $E2$ have meanings as discussed in Section 2.4. If $\hat{\text{SII}}$ is greater than the previously recorded MaxSII value, set MaxSII to $\hat{\text{SII}}$, and set $\hat{k}_{\text{MSII}}$ to t.

Step 5 increment t, goto Step 2 if $t \leq 253$; otherwise goto Step 6

Step 6 the MaxSII variable holds the estimated maximum SII value, and the $\hat{k}_{\text{MSII}}$ value is the optimum threshold value.

Note that for the thresholding of a real image, the subimage pdfs $f_0(g)$, $f_1(g)$, and the mixing ratio α are unknown. They are estimated in Step 3 and the SII at threshold t is estimated in Step 4.

To assess the performance of the MSII thresholding algorithm, we employ it to threshold images in four different cases. In the first case, we have chosen to threshold three synthetic ideal pdfs that have been studied by some authors [13]. In the second case, the same set of ideal pdfs that have been synthesized in Section 3.2 of this paper are thresholded. In the third case, a blurred and noisy synthetic image is thresholded. In the fourth case, two real images are thresholded. For the first three cases, the thresholding results are compared to the ideal threshold values k_{MINE}, k_{MSII}, k_{UNFE}, as well as threshold values obtained by four other well-known thresholding algorithms, namely Otsu's (OTSU) algorithm [26], Wong and Sahoo's maximum entropy (ME) algorithm [5], Kittler and Illingworth's minimum error (KIT) algorithm [21], and Li and Lee's minimum cross entropy (MCE) algorithm [13]. For the fourth case, the thresholding results are assessed mainly by visual inspection.

In the first case, the image parameters and the thresholding results of thresholding three synthetic ideal pdfs are summarized in Table 1. Among the five thresholding algorithms, the MSII algorithm and the KIT algorithm perform substantially better than the other three algorithms. The MSII algorithm achieves threshold values close to the ideal MSII threshold values, and the KIT algorithm is able to achive threshold values close to the ideal MINE threshold values. The MSII and the KIT algorithms have been equally accurate in thresholding these three synthetic images, and their results are very near to the ideal thresholding results. Very good performance has been demonstrated. The MSII and KIT algorithms are designed by assuming that the image pdf is a mixture of two normal distributions, and the images to be thresholded in this case have been synthesized by mixing two normal distribution. Hence, it is not surprising that good thresholding results have been obtained by the KIT and the MSII algorithms for these synthesized images.

In the second case, we threshold 7078 ideal pdfs which are obtained by discarding 103 images having ideal MINE threshold values of -1 from those 7181 ideal pdfs obtained in Section 3.2. These 103 ideal pdfs are not considered for performance comparison because they represent cases for which the MINE thresholding criterion fails. In order to assess how well a thresholding algorithm can meet the MSII, MINE, and UNFE criteria, the root-mean-square difference between threshold values obtained by each of the five thresholding algorithms and the ideal MINE, MSII, and UNFE threshold values are computed separately over the set of 7078 ideal pdfs. The results are summarized in Table 2. It can be seen that all five algorithms meet the ideal MSII thresholding criterion better than they do for the ideal MINE and ideal UNFE criteria. In particular, the

TABLE 1
Comparison of Performance of Thresholding Algorithms for Three Ideal pdfs

	Image parameters $(\alpha, \mu_0, \sigma_0, \mu_1, \sigma_1) =$ (0.25, 38, 9, 121, 44)	Image parameters $(\alpha, \mu_0, \sigma_0, \mu_1, \sigma_1) =$ (0.45, 47, 13, 144, 25)	Image parameters $(\alpha, \mu_0, \sigma_0, \mu_1, \sigma_1) =$ (0.5, 50, 4, 150, 30)
Ideal MINE threshold value	54	81	63
Ideal MSII threshold value	58	82	64
Ideal UNFE threshold value	52	80	61
OTSU threshold value	98	97	102
ME threshold value	129	117	164
KIT threshold value	60	82	64
MCE threshold value	82	87	92
MSII threshold value	58	82	63

TABLE 2
Average Performance of Thresholding Algorithms on 7078 Ideal pdfs

	R.M.S. threshold error between ideal MINE thresholds	R.M.S. threshold error between ideal MSII thresholds	R.M.S. threshold error between ideal UNFE thresholds	Success rate
MSII algorithm	17.20	6.87	12.15	100%
KIT algorithm	10.18	8.57	14.46	42%
OTSU algorithm	28.21	18.30	21.21	100%
MCE algorithm	24.13	16.08	21.86	100%
ME algorithm	24.39	18.60	25.69	100%

MSII algorithm is the most accurate in meeting the ideal MSII and UNFE criteria, and the KIT algorithm is the most accurate in meeting the ideal MINE criterion. Except for the KIT algorithm, all the other four algorithms have been successful in finding a threshold value within the gray-level value range of [0, 255] for each of the 7078 ideal pdfs. The KIT algorithm can threshold only 2996 of the 7078 ideal pdfs. This may be the reason why the KIT algorithm appears to meet the ideal MINE criterion better, since it simply fails rather than giving an inaccurate threshold value for a large number of images; the failure cases are not taken into account when the r.m.s. differences among the threshold values are computed. For a fair comparison to be made, we also compute the r.m.s. threshold values differences over these 2996 ideal pdfs that have been successfully thresholded by the KIT algorithm. The results are summarized in Table 3. For the OTSU, MCE, and ME algorithms, there is not much change in average thresholding accuracy. For the MSII algorithm, the average thresholding accuracy over these 2996 images has improved substantially such that it becomes better than the KIT algorithm.

In the third case, a blurred and noisy image is synthesized and thresholded by the algorithms. This experiment investigates how the algorithms would perform when applied to synthetic images when pdf is not a simple mixture of two Gaussian pdfs. The method of synthesizing the image is similar to that discussed in [27]. The scene is an ellipse in a background. The ellipse has a relative size of 0.2 with respect to the entire image size and an aspect ratio of 1.5. For the gray-scale image, all the ellipse pixels have a gray-level value of 100 and all the background pixels have a gray-level value of 160. The gray-scale image is convolved with a 3×3 uniform mask to create a blurring effect. After the blurring, a Gaussian noise with zero mean and standard deviation of 20 is added to the gray-scale image by a random number generation subroutine [25] that generates Gaussian distributed random integers in the gray-level value range of [0, 255]. The final result is a blurred, noisy image as shown in Fig. 4a. Its histogram is shown in Fig. 4b. The scene entropy $H(X)$ of this image is 0.7283 bits/pixel, and the gray-scale image information (GII) of this image is 0.5352 bits/pixel, about 73.5% of $H(X)$. From the information-theoretic point of view, this gray-scale image is not a very good image for segmentation since the GII is not very large. From the previous discussion about the relationship between $H(X)$, GII, and segmented image information (SII), it would be anticipated that for this image, any pdf-based thresholding algorithm will produce a segmented image with SII smaller than the GII, i.e., smaller than 0.5352 bits/pixel. When the KIT algorithm is applied, no internal minimum can be determined and hence no threshold value can be obtained. The thresholding results of the remaining four thresholding algorithms are summarized in Table 4, where the threshold values, the segmentation eror rate, and the SII are tabulated. From these results, it can be seen that the MSII algorithm performs best among all other algorithms in that it achieves the smallest segmentation error rate and the largest SII. The ME algorithm performs the second best. The four thresholded images are shown in Figs. 4c–4f. From this example, it is shown that the MSII thresholding algorithm is able to achieve good thresholding results for a blurred and noisy image.

TABLE 3
Average Performance of Thresholding Algorithms on 2996 Ideal pdfs

	R.M.S. threshold error between ideal MINE thresholds	R.M.S. threshold error between ideal MSII thresholds	R.M.S. threshold error between ideal UNFE thresholds	Success rate
MSII algorithm	7.73	4.64	7.92	100%
KIT algorithm	10.18	8.57	14.46	100%
OTSU algorithm	21.65	18.47	23.84	100%
MCE algorithm	20.37	18.04	23.84	100%
ME algorithm	28.26	25.37	29.38	100%

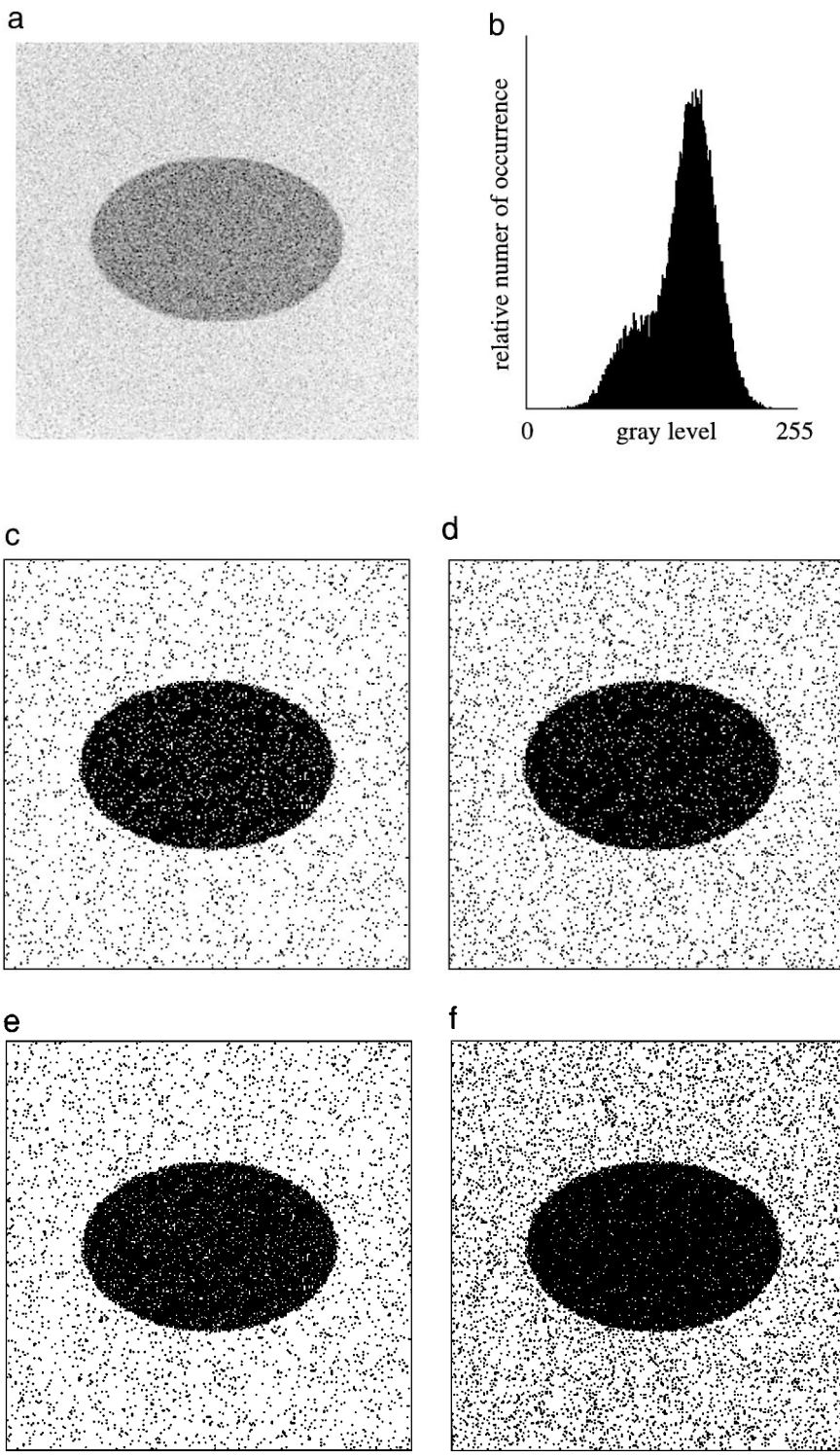

FIG. 4. Thresholding results for an ellipse, image parameters are $\alpha = 0.2$, $\mu_0 = 100$ and $\mu_1 = 169$, blurred by 3×3 uniform mask and corrupted by Gaussian noise with standard deviation of 20: (a) blurred and noisy gray-scale image, (b) histogram, (c) thresholded by MSII algorithm at 126, (d) thresholded by MCE algorithm at 130, (e) thresholded by ME algorithm at 127, (f) thresholded by OTSU algorithm at 135.

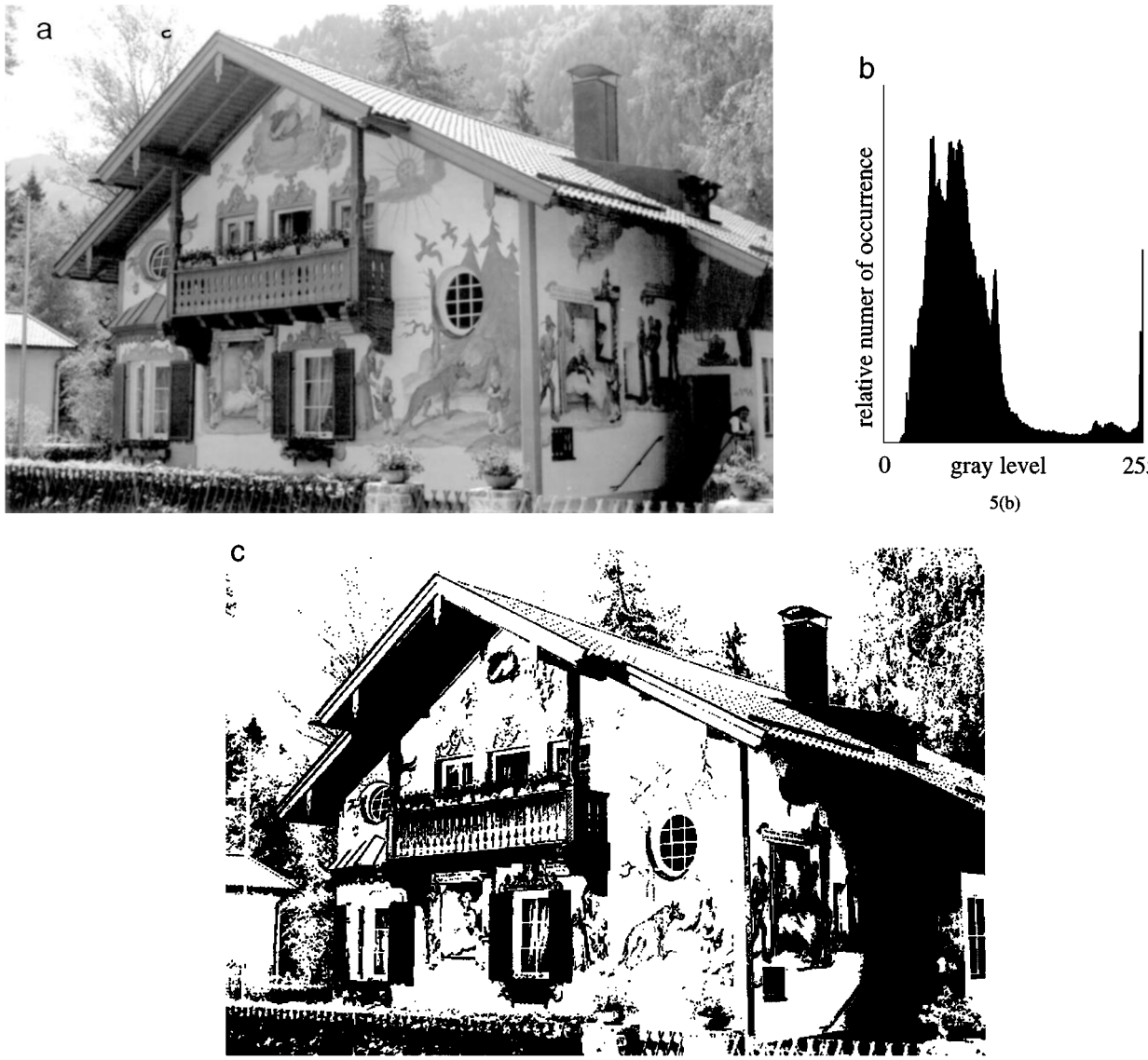

FIG. 5. Thresholding results of a real image: (a) gray-scale image, (b) histogram, (c) thresholded by MSII algorithm at 64, (d) thresholded by MCE algorithm at 91, (e) thresholded by ME algorithm at 118, (f) thresholded by OTSU algorithm at 141, (g) thresholded by a manually chosen threshold value suggested by KIT algorithm at 180.

In the fourth case, we employ the MSII algorithm to threshold three real images and compare the thresholding results obtained by the other four thresholding algorithms. Since no *a priori* image modeling knowledge is known for these real images, no ideal threshold values can be found and hence no objective and quantitative assessment on the thresholding performance can be made. The assessment we make on the performance of the five algorithms is mainly by visual inspection. The first real image to be thresholded is a monochrome image in a 768×512 pixels format. Each gray-level value is quantized in 8 bits, ranging from 0 to 255 inclusive. The gray-scale image and its histogram are shown in Figs. 5a and 5b, respectively. The MSII, MCE, ME, and OTSU algorithms give a threshold value of 64, 91, 118, and 141, respectively. The KIT algorithm results in two internal minima, corresponding to threshold values of 180 and 247, hence the KIT algorithm suggests two possible threshold values for this image. Based on a subjective viewing of the two possible thresholding results, better thresholding result is obtained when the image is thresholded at 180 rather than at 247. Hence, a threshold value of 180 is chosen manually to be the solution of the KIT algorithm. The five thresholded images are shown in Figs. 5c–5g. Based on visual inspection, it can be seen that the thresholded images by the MSII and MCE algorithms contain many identifiable features of the scene. For the other three algorithms, not many such features can be found in the thresholded images. Comparatively speaking, the thresholding results by the MSII and the MCE algorithms are better among the five. But it is difficult to comment further whether the MSII

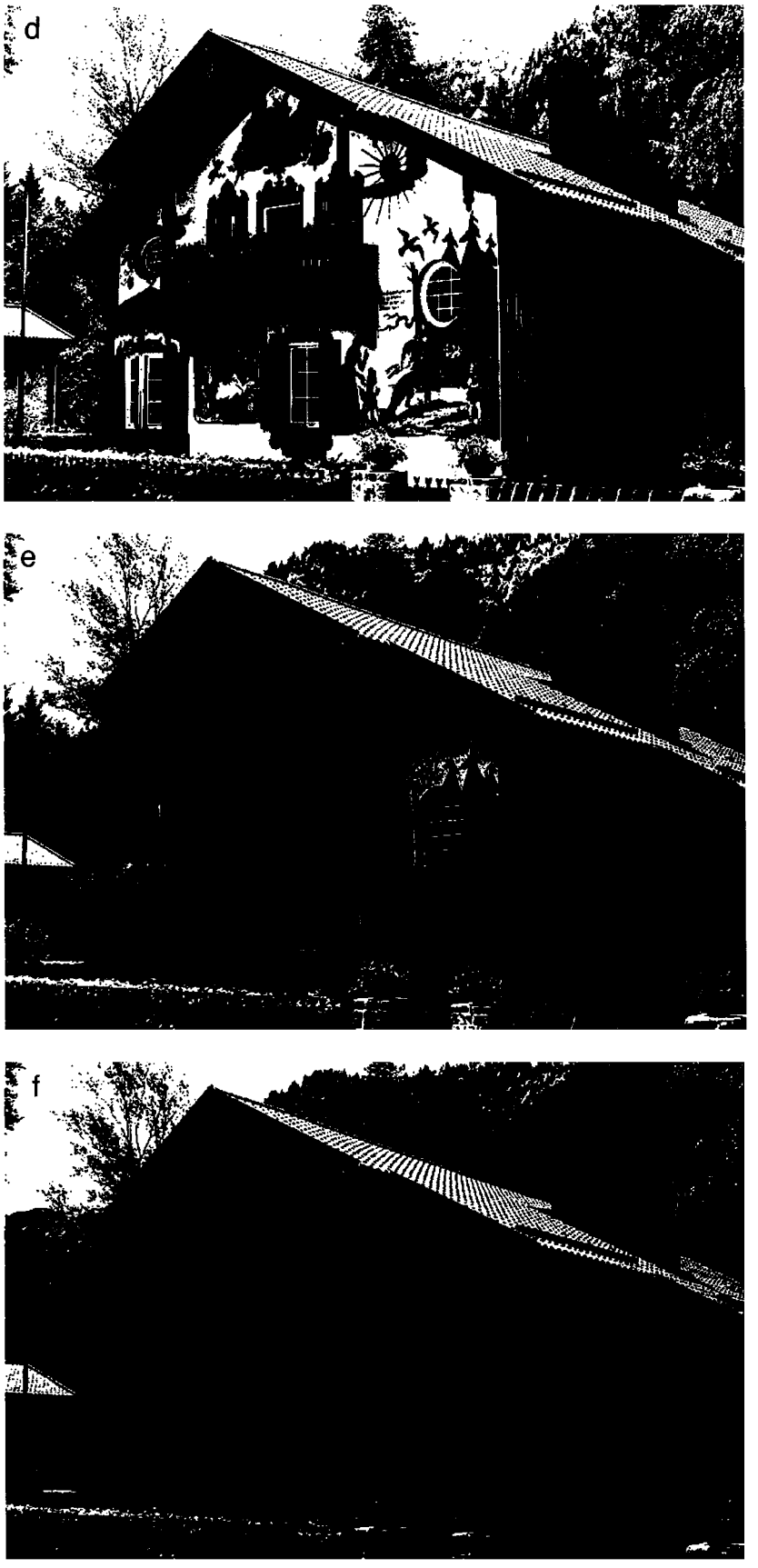

FIG. 5—*Continued*

FIG. 5—*Continued*

algorithm performs better than the MCE algorithm, or the other way round. A judgment of this kind depends on what features of the scene one is interested in; hence, it is application-dependent. But as an assessment of the MSII algorithm, this result demonstrates that it is capable of finding a satisfactory threshold value for a complicated real image.

The second real image to be thresholded is an image containing four airplanes in a background. This image is typical of one that has several similar objects in a homogenous background. This monochrome image has a size of 256 × 256 pixels and 8-bit resolution in the gray-level values. The gray-scale image and its histogram are shown in Figs. 6a and 6b, respectively. The threshold values determined by the MSII, MCE, ME, OTSU, and KIT algorithms are, respectively, 125, 157, 128, 160, and 44. The five thresholded images are presented in Figs. 6c–6g. If the purpose of thresholding this image is to make the four planes identifiable, the thresholded image by the KIT algorithm is too bright, while the thresholded images by the MCE and the OTSU algorithms are too dark, such that the planes are confused by the smokes emitted. The thresholded images by the MSII and the ME algorithms are satisfactory since the four planes are clearly identifiable. However, if the purpose of thresholding is to identify the emission level of the jet engines rather than the planes in order to assess the pollution level, then the thresholded images by the MCE and the OTSU algorithms would be better. This example shows that the MSII algorithm (and the ME algorithm) is able to segment out the flying planes, which are objects in a uniform background. This type of image is commonly encountered in many image-segmentation applications.

TABLE 4
Thresholding Results for a Blurred and Noisy Image

	Threshold value	Segmented error	Segmented image information
MSII algorithm	126	5.83%	0.4455 bits/pixel
OTSU algorithm	135	9.62%	0.4091 bits/pixel
MCE algorithm	130	7.06%	0.4363 bits/pixel
ME algorithm	127	6.04%	0.4449 bits/pixel
KIT algorithm	No value obtained	—	—

The third real image to be thresholded is an image which has a size of 256 × 256 pixels and 8-bit resolution for the gray-level values. The gray-scale image and its histogram are shown in Figs. 7a and 7b, respectively. The threshold values determined by the MSII, MCE, ME, OTSU, and KIT algorithms are 79, 74, 124, 82, and 223, respectively. The five thresholded images are presented in Figs. 7c–7g. It can be seen that the performance of MCE, MSII, and OTSU algorithms is similar. Although the image is quite complicated in content, the thresholded images still possess details, such as the flower and the leaves of the scene. The ME and KIT algorithms have thresholded the image too dark, with many details of the scene lost. This example shows that the MSII algorithm (and the MCE and OTSU algorithms as well) is able to threshold an image with complicated contents while preserving substantial details about the scene.

5. DISCUSSION

Although only two-class thresholding has been discussed in the previous sections, we remark here that the concept of MSII

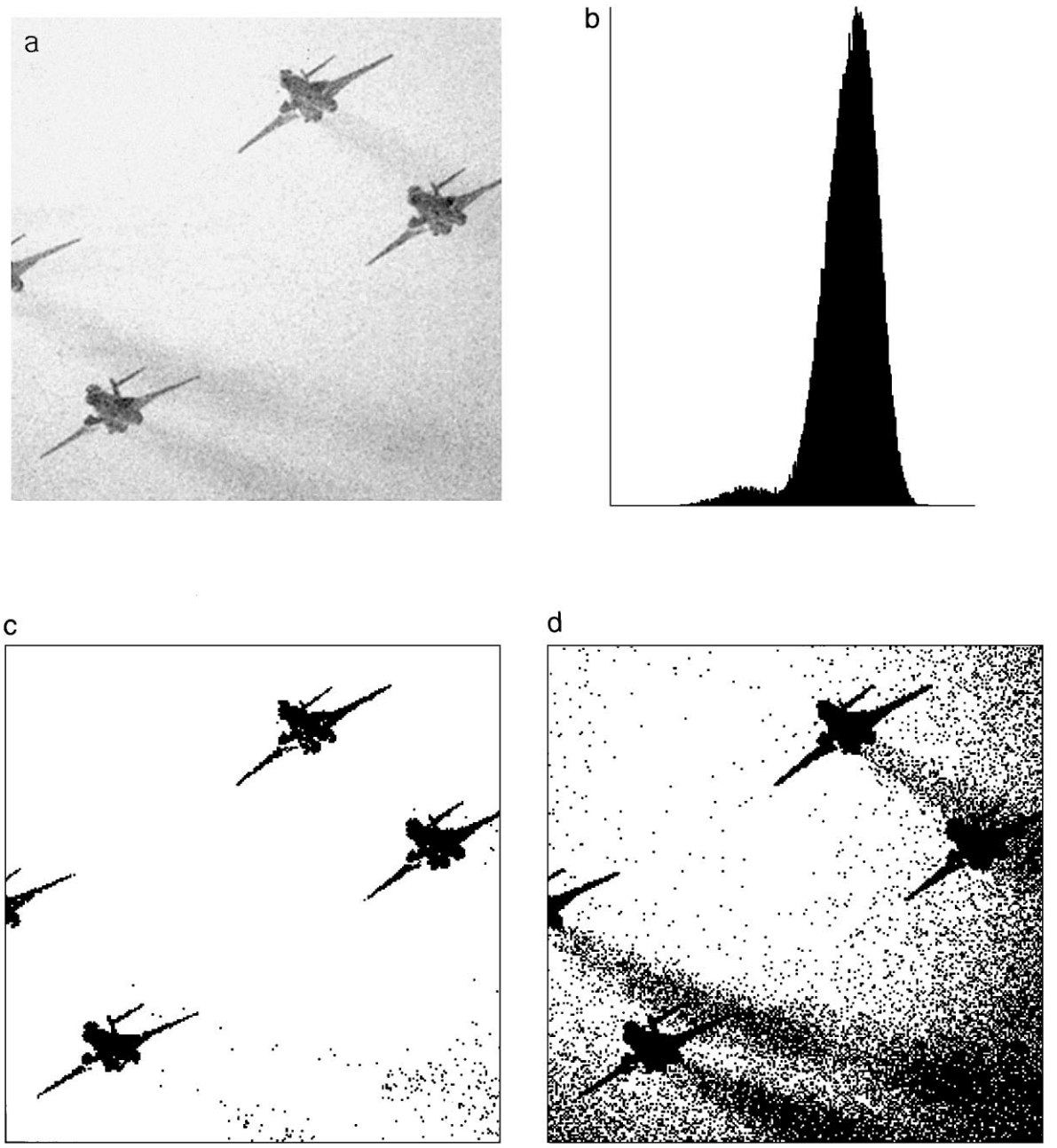

FIG. 6. Thresholding results of a real image: (a) gray-scale image, (b) histogram, (c) thresholded by MSII algorithm at 125, (d) thresholded by MCE algorithm at 157, (e) thresholded by ME algorithm at 128, (f) thresholded by OTSU algorithm at 160, (g) thresholded by KIT algorithm at 44.

thresholding is readily extendable to the multiclass situation. Consider that a scene consists of r objects in a background. The image is composed of $r + 1$ classes of pixels, where each class is denoted as F_j, and each has a gray-level value pdf of $f_j(g)$, for $j = 0, 1, \ldots, r$. Suppose that the size of the F_j class relative to the entire image is α_j. The pdf of the composite image is given by $f(g) = \alpha_0 f_0(g) + \alpha_1 f_1(g) + \cdots + \alpha_r f_r(g)$. Using notations similar to those employed in the previous sections, it may be shown that the scene entropy, the gray-scale image information, and the segmented image information are, respectively, given in

$$H(X) = H_{r+1}[\alpha_0, \alpha_1, \ldots, \alpha_r] \tag{27}$$

$$\mathrm{GII} = H(F) - \sum_{j=0}^{r} \alpha_j H(F_j) \tag{28}$$

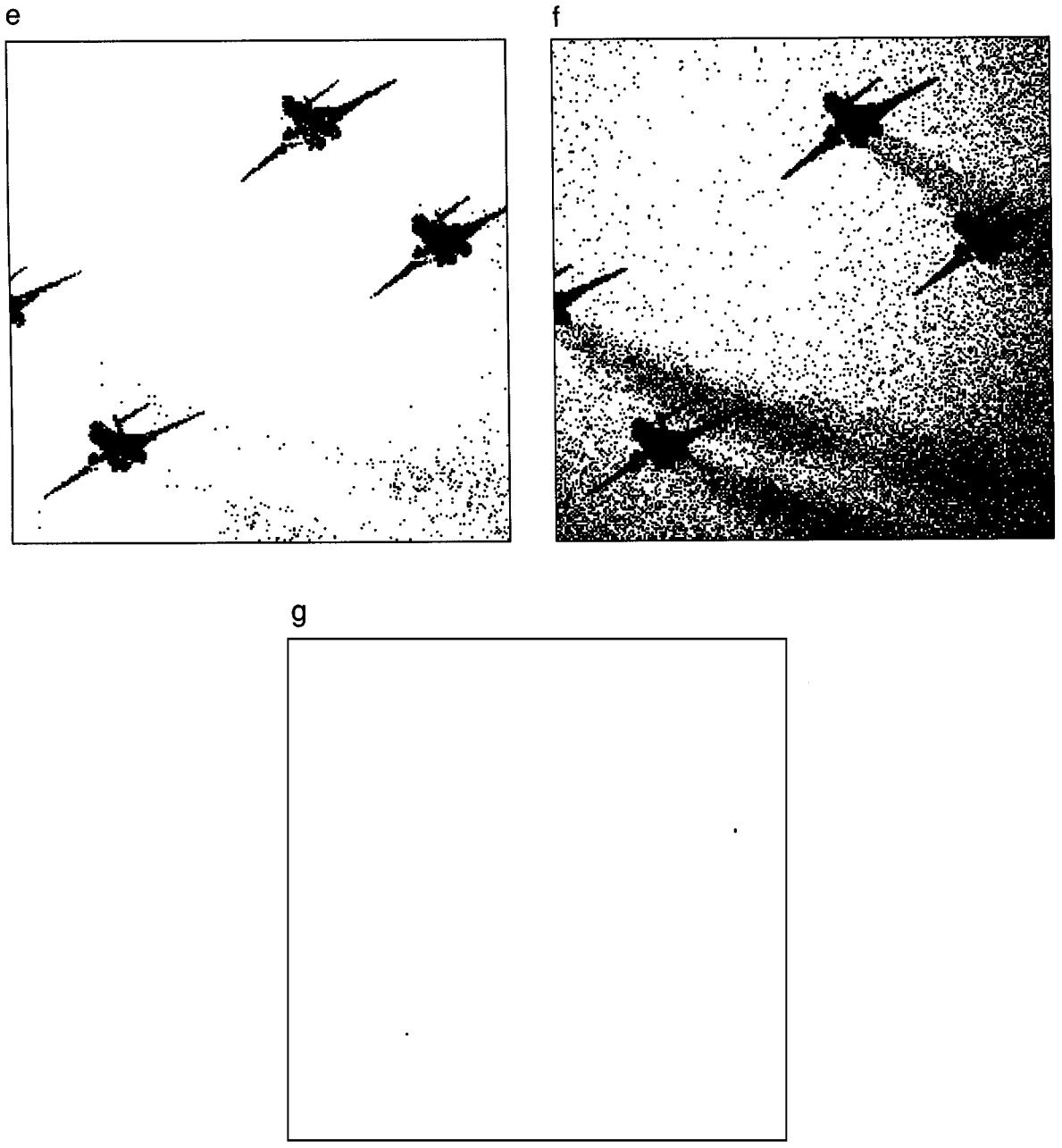

FIG. 6—*Continued*

$$\mathrm{SII} = H_{r+1}[P_0, P_1, \ldots, P_r] - \sum_{j=0}^{r} \alpha_j H_{r+1}[P_{0j}, P_{1j}, \ldots, P_{rj}]. \tag{29}$$

Due to the similarities in their structures, it may be easily recognized that Eqs. (27), (28), and (29) are multiclass extensions of Eqs. (3), (9), and (16), respectively. For the case of $(r+1)$-class MSII thresholding, the criterion function SII_k is maximized by choosing the optimum vector $\boldsymbol{k} = (k_1, k_2, \ldots, k_r)$, which is a collection of r threshold values.

6. CONCLUSION

The image segmentation process is analyzed in a communication perspective that considers the amount of information transferred to an observer by way of a segmented image. Based on this communication perspective, a thresholding criterion, maximum segmented image information, that maximizes the amount of information contained in a segmented image, is proposed and described. By studying the thresholding results of a large number of synthetic images, it is found that the ideal MSII threshold values always lie within the gray-level value

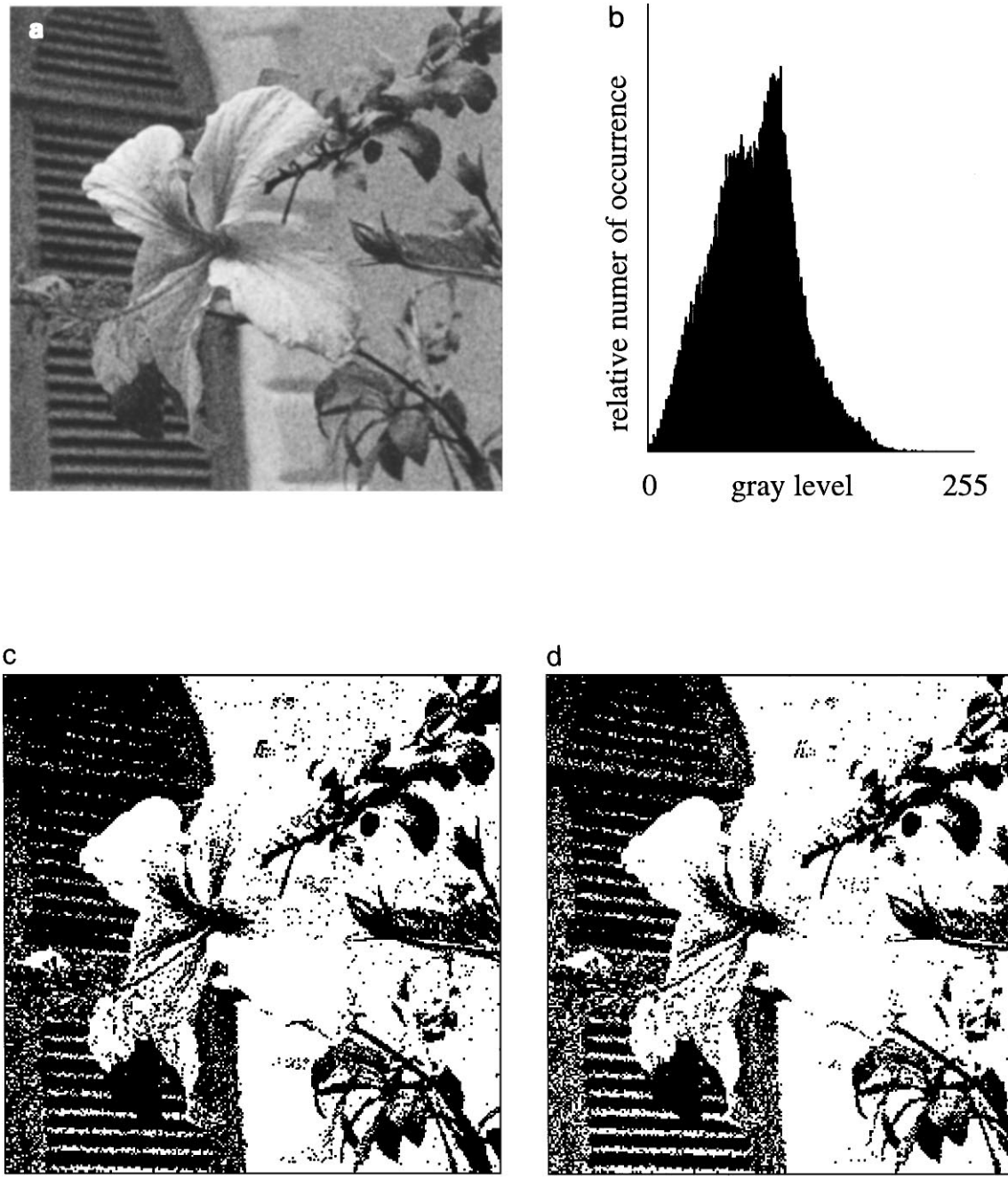

FIG. 7. Thresholding results of a real image: (a) gray-scale image, (b) histogram, (c) thresholded by MSII algorithm at 79, (d) thresholded by MCE algorithm at 74, (e) thresholded by ME algorithm at 124, (f) thresholded by OTSU algorithm at 82, (g) thresholded by KIT algorithm at 223.

range, and hence always exist. Thus, the MSII thresholding criterion is compatible with the *a priori* assumption that the image is composed of one or more objects in a background. Under a comparison study, the ideal MSII threshold values are found to lie close to the ideal minimum error and the ideal uniform error threshold values. For thresholding real images, a thresholding algorithm based on the MSII thresholding criterion is proposed and evaluated. This algorithm is known as the *MSII thresholding algorithm*. Based on the thresholding results for a large number of synthetic images, the MSII algorithm is able to find threshold values for all the images under study. Furthermore, it is found that the MSII thresholding algorithm is more accurate than other thresholding algorithms in the comparison study. When two real images are thresholded in the study, the thresholded images obtained by the MSII algorithm contain many identifiable features of the original scene, hence good thresholding results have been obtained. Finally, it is shown that the MSII concept is readily extendable to threshold

FIG. 7—*Continued*

multiclass images. In view of its compatibility with *a priori* information, high accuracy, high success rate, and extendability to multiclass thresholding, the MSII approach is suitable for image thresholding.

REFERENCES

1. C. E. Shannon and W. Weaver, *The Mathematical Theory of Communication*, University of Illinois Press, Urbana, 1964.
2. A. Rosenfeld and A. Kak, *Digital Picture Processing*, 2nd ed., Academic Press, New York, 1982.
3. P. K. Sahoo, S. Soltani, A. K. C. Wong, and Y. C. Chen, A survey of thresholding techniques, *Comput. Vision Graphics Image Process.* **41**, 1988, 233–260.
4. T. Pun, A new method for grey-level picture thresholding using the entropy of the histogram, *Signal Process.* **2**, 1980, 223–237.
5. A. K. C. Wong and P. K. Sahoo, A gray-level threshold selection method based on maximum entropy principle, *IEEE Trans. Systems Man Cybern.* **19**(4), 1989, 866–871.
6. N. R. Pal and S. K. Pal, Entropic thresholding, *Signal Process.* **16**, 1989, 97–108.
7. N. R. Pal and S. K. Pal, Entropy: a new definition and its applications, *IEEE Trans. Systems Man Cybern.* **21**(5), 1991, 1260–1270.

8. A. Beghdadi, A. L. Negrate, and P. V. D. Lesegno, Entropic thresholding using a block source model, *CVGIP: Graphical Models and Image Process*. **57**, 1995, 197–205.
9. G. Johannsen and J. Bille, A threshold selection method using information measures, in *Proceedings, 6th Int. Conf. Pattern Recognition, Munich, Germany, 1982*, pp. 140–142.
10. J. N. Kapur, P. K. Sahoo, and A. K. C. Wong, A new method for gray-level picture thresholding using the entropy of the histogram, *Comput. Vision Graphics Image Process*. **29**, 1985, 273–285.
11. A. S. Abutaleb, Automatic thresholding of gray-level pictures using two-dimensional entropy, *Comput. Vision Graphics Image Process*. **47**, 1989, 22–32.
12. A. Brink, Maximum entropy segmentation based on the autocorrelation function of the image histogram, *J. Comput. Inform. Technol*. **2**(2), 1994, 77–85.
13. C. H. Li and C. K. Lee, Minimum cross entropy thresholding, *Pattern Recognit.* **26**, 1993, 617–625.
14. C. I. Chang, K. Chen, J. Wang, and M. L. G. Althouse, A relative entropy-based approach to image thresholding, *Pattern Recognition* **27**, 1994, 1275–1289.
15. F. K. Lam and C. K. Leung, Image segmentation using maximum entropy method, in *Proceedings, Int. Sym. Speech, Image Process. and Neural Networks, Hong Kong, 1994*, pp. 29–32.
16. R. W. Hamming, *Coding and Information Theory*, Prentice Hall, New Jersey, 1980.
17. A. Feinstein, *Foundations of Information Theory*, McGraw–Hill, New York, 1958.
18. R. M. Haralick and L. Shapiro, *Computer and Robot Vision*, Vol. I, Addison-Wesley, Reading, MA, 1992.
19. S. Venkatesh and P. L. Rosin, Dynamic threshold determination by local and global edge evaluation, *Graphical Models Image Process.* **57**(2), 1995, 146–160.
20. S. M. Dunn, D. Harwood, and L. S. Davis, Local estimation of the uniform error threshold, *IEEE Trans. Pattern Anal. Machine Intell*. **1**(6), 1984, 742–747.
21. J. Kittler and J. Illingworth, Minimum error thresholding, *Pattern Recognition* **19**, 1986, 41–47.
22. Y. Nakagawa and A. Rosenfeld, Some experiments on variable thresholding, *Pattern Recognition* **11**, 1979, 191–204.
23. T. Kurita, N. Otsu, and N. Abdelmalek, Maximum likelihood thresholding based on population mixture models, *Pattern Recognition* **25**, 1992, 1231–1240.
24. C. A. Glasbey, An analysis of histogram-based thresholding algorithms, *CVGIP: Graphical Models Image Process*. **55**, 1993, 532–537.
25. D. E. Knuth, *The Art of Computer Programming, Vol. 2: Seminumerical Algorithms*, 2nd ed., Addison-Wesley, Reading, MA, 1981.
26. N. Otsu, A threshold selection method from gray-level histograms, *IEEE Trans. Systems Man Cybern.* **9**(1), 1979, 62–66.
27. Y. J. Zhang and J. J. Gerbrands, Objective and quantitative segmentation evaluation and comparison, *Signal Process*. **39**, 1994, 43–54.